Effect of substrate miscut angle on critical thickness, structural and electronic properties of MBE-grown NbN films on c-plane sapphire

Cite as: Appl. Phys. Lett. **128**, 042602 (2026); doi: 10.1063/5.0312575
Submitted: 17 November 2025 · Accepted: 7 January 2026 ·
Published Online: 30 January 2026

View Online Export Citation CrossMark

Anand Ithepalli,[1] Saumya Vashishtha,[2] Naomi Pieczulewski,[1] Qiao Liu,[1] Amit Rohan Rajapurohita,[2] Matthew Barone,[1] Darrell Schlom,[1,3,4] David A. Muller,[2,3] Huili Grace Xing,[1,3,5] and Debdeep Jena[1,3,5,a)]

AFFILIATIONS

[1]Department of Materials Science and Engineering, Cornell University, Ithaca, New York 14850, USA
[2]School of Applied and Engineering Physics, Cornell University, Ithaca, New York 14850, USA
[3]Kavli Institute at Cornell for Nanoscale Science, Cornell University, Ithaca, New York 14850, USA
[4]Leibniz-Institut für Kristallzuchtüng, Max-Born-Str.. 2, 12489 Berlin, Germany
[5]School of Electrical and Computer Engineering, Cornell University, Ithaca, New York 14850, USA

[a)]**Author to whom correspondence should be addressed:** djena@cornell.edu

ABSTRACT

We report the structural and electronic properties of niobium nitride (NbN) thin films grown by molecular beam epitaxy on c-plane sapphire with miscut angles of 0.5°, 2°, 4°, and 10° toward m-axis. X-ray diffraction scans reveal that the full width at half maximum of the rocking curves around the 1 1 1 reflection of these NbN films decreases with increasing miscut. Starting from 76 arcsecs on 0.5° miscut, the FWHM reduces to almost 20 arcsecs on 10° miscut sapphire, indicating improved structural quality. Scanning transmission electron microscopy images indicate that NbN on c-sapphire has around 10 nm critical thickness, irrespective of the substrate miscut, above which it turns columnar. The improved structural property is correlated with a marginal increment in superconducting transition temperature T_c from 12.1 K for NbN on 0.5° miscut sapphire to 12.5 K for NbN on 10° miscut sapphire.

Since the discovery of its superconductivity in 1941,[1] niobium nitride has gained a lot of interest. Brauer identified the multiple structural phases, each with a characteristic Nb:N ratio, in the niobium–nitrogen binary phase diagram.[2] The superconducting transition temperature of niobium nitride varies in the range $0.4\,\text{K} \leq T_c \leq 17.3\,\text{K}$, typically increasing with increasing N:Nb ratio.[3–7] Epitaxial growth of thin films of niobium nitride on various substrates has been extensively reported.[4,8–15] This work is focused on c-plane sapphire, which is widely used for quantum applications owing to its low dielectric loss of sapphire.[16] Wright *et al.* discussed the growth windows of phase-pure niobium nitride films on c-plane sapphire substrate using plasma-assisted molecular beam epitaxy (PAMBE).[4] The rock salt phase of niobium nitride, referred to as δ-NbN, with a Nb:N stoichiometry around 1:1 has the highest T_c among all the pure niobium nitride phases in bulk form.[3] Wright *et al.* confirmed that among phase-pure niobium nitride thin films, δ-NbN has the highest T_c around 13 K when grown on c-sapphire using PAMBE. Despite having the highest T_c, δ-NbN showed 3-dimensional island growth mode and twinning due to symmetry mismatch with the c-plane sapphire substrate, resulting in broad rocking curves (RCs) around the symmetric x-ray diffraction (XRD) peaks with full width at half maximum (FWHM) reaching 200 arcsecs.[4]

In this report, we attempt to answer the following question: Can the structural quality of MBE-grown δ-NbN on c-plane sapphire substrate be further improved? The use of high miscut substrates is identified as a possible solution. For instance, Nagai had shown improvement in the structural quality of $In_xGa_{1-x}As$ films grown on optimal miscut angles of GaAs substrates.[17] He discovered that the planes of the $In_xGa_{1-x}As$ film were tilted with respect to the planes of GaAs due to the difference in their inter-planar spacings as shown in Fig. 1. He attributed the structural improvement to the epitaxial tilt which reduces the nucleation degrees of freedom, due to the terrace widths being smaller than the nucleating grain sizes, resulting in a reduction in the twin and anti-phase domains. Domain boundaries

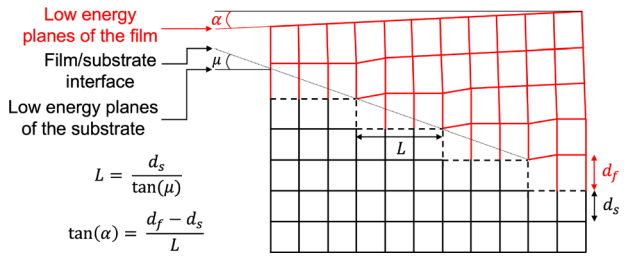

FIG. 1. Schematic of the Nagai tilt. Substrates with a miscut angle μ form terraces with atomic steps on the surface to lower the surface energy. The terrace width L depends on the miscut angle and the step height d_s which is the inter-planar spacing of the low energy planes. The difference in the inter-planar spacings of the film d_f and the substrate d_s causes an epitaxial tilt α, which is the angle between the low energy planes of the film and the substrate.

and mosaicity are expected to reduce with increasing miscut angle. This is because miscut adds a constraint on the various degrees of freedom of nucleation. As an example, a threefold symmetric plane has two degrees of freedom for nucleation on a sixfold symmetric plane. Miscut along one direction breaks the degeneracy of these two twins. A similar argument may be made for mosaic tilts.

The epitaxial tilt is observed in many material systems since Nagai's report. Among nitrides, a recent example of Nagai tilt is shown in aluminum gallium nitride ternary alloy thin films grown on large miscut aluminum nitride substrates.[18] Further, reduction of defects such as the surface hillocks on N-polar gallium nitride (GaN) grown on c-sapphire[19] and on N-polar GaN single crystals[20] has been achieved by employing large miscut substrates.

Motivated by the Nagai tilt induced reduction of defects, δ-NbN was grown on c-sapphire with four different miscut angles of 0.5°, 2°, 4°, 10° along the m-axis. Such large miscut substrates are difficult to obtain, and for this study, specially prepared wafers by Kyocera Inc. were used. To avoid experimental discrepancies due to growth-to-growth variations, all substrates with various miscut angles were co-loaded on a lapped silicon carrier wafer using indium mounting. Using a nitrogen plasma source and Nb from an E-beam source in a PAMBE system, around 40 nm δ-NbN was then deposited on the co-loaded substrates with an active N-to-Nb flux ratio of 2:1 at a substrate temperature of 600 °C measured by a thermocouple. The growth conditions are similar to that reported by Wright *et al.*[4] A control set of δ-NbN was also grown on 4 identical c-sapphire substrates with 0.5° miscut. We refer to δ-NbN as NbN in the rest of this report and discuss the evidence of phase-purity.

Coupled symmetric XRD scans around the 1 1 1 reflection of NbN on sapphire substrates with miscut angles of 0.5°, 2°, 4°, and 10° are shown in Fig. 2 along with the bulk NbN 1 1 1 peak location at $2\theta = 35.4°$. The NbN film experiences an in-plane tensile strain.[21] Such a strain induces an out-of-plane compressive strain related through the film's Poisson ratio, ν. An out-of-plane compressive strain results in an increasing Bragg angle in XRD. The primary NbN 1 1 1 reflection shifts closer to its bulk value of 35.4° as the substrate miscut is increased. This may be interpreted as reduction in strain because our films have single NbN phase as discussed later in the text. Interestingly, with increasing substrate miscut, the NbN 1 1 1 reflection peak width becomes narrower. A shoulder peak with similar width persists across different miscuts, potentially due to the partially

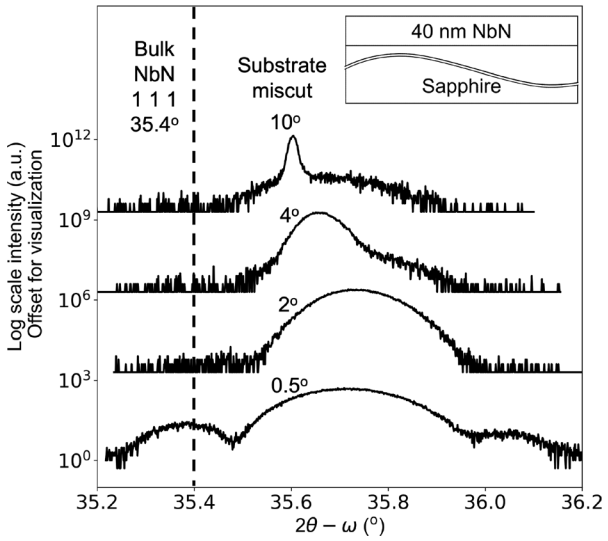

FIG. 2. Symmetric 2θ–ω coupled scans around $2\theta = 35.4°$ expected for NbN 1 1 1 peak after aligning the instrument to NbN 1 1 1 reflection show narrower peaks with increasing miscut angle of the substrate and the peak position shifts closer toward the bulk NbN peak position.

strained NbN below critical thickness. The FWHM of the primary $2\theta - \omega$ peaks around NbN 1 1 1 reflection reduces from 727.2″ on the 0.5° miscut substrate to 57.6″ on the 10° miscut substrate. In contrast, there is no difference in the XRD scans of the control set of NbN films on the same miscut substrate as shown in the supplementary material, Fig. S1.

The broadening of $2\theta - \omega$ XRD peaks is typically attributed to crystallite/grain sizes and micro-strain following the Williamson–Hall equation,[22] $\beta\cos(\theta) = k\lambda/L + 4\epsilon\sin(\theta)$, where β is the FWHM of the diffraction peak at the diffraction angle 2θ, k is the shape factor usually around 0.9, λ is the wavelength of the x-ray source, L is the crystallite size, and ϵ is the strain. As is shown later in this manuscript using scanning transmission electron microscopy (STEM), the NbN columnar grain sizes are similar for substrate miscut of 0.5° and 10°, whereas β changes by a factor of more than 12. Therefore, the Williamson–Hall equation reduces to $\beta \propto \epsilon$, implying that the strain in NbN grown on higher miscut substrate is lower. This is also evident from the shift in primary NbN 1 1 1 reflection as the substrate miscut is increased. *What is the cause for the reduction in strain?* One possible explanation for this reduction in strain is a reduction in nitrogen vacancies. Signatures of reduction in N-vacancies by employing a higher miscut substrate were also observed by Tatarczak *et al.* in gallium nitride homoepitaxial layers via photoluminescence measurements.[23] Figure S2 in the supplementary material also supports the argument that the XRD peak shifts to a lower Bragg angle as the N:Nb ratio is increased albeit with a change in the structural phase.

The other possibility for change in strain is a change in the structural phase of niobium nitride. Structural phases in the Nb-N binary phase diagram have been studied extensively over the last few decades.[2,4,10,24–26] The hexagonal niobium nitride phases, ϵ-NbN and β-Nb_2N, are easy to identify and distinguish from δ-NbN using x-ray diffraction, electron microscopy, and superconducting transition

temperature. The experimental data provided in this manuscript cross out any possibility of inclusions of these hexagonal phases. However, a similar phase as δ-NbN with 25% ordered N-vacancy, namely, γ-Nb_4N_3, is difficult to distinguish from δ-NbN. Due to the low free energy difference between γ-Nb_4N_3 and δ-NbN,[26] there is a possible continuous phase transformation[24,25] between these two phases.

The unit cells of γ-Nb_4N_3 and δ-NbN are compared with each other in the supplementary material, Fig. S3, to show the similarities between these two phases and how XRD can help distinguish them. The absence of γ-Nb_4N_3 phase in our films is verified using reciprocal space maps shown in the supplementary material, Fig. S4. This rules out the possibility of structural phase change due to change in substrate miscut leading to a change in the strain of the film. The Nb:N ratio of 1:1 is not guaranteed even though the structural phase is shown to be that of δ-NbN. As pointed out in earlier studies, disordered N-vacancies in δ-NbN are symmetry preserving.[24–26] Therefore, reduction in N-vacancies remains a plausible mechanism for the observed XRD differences.

Figure 3 shows the normalized and centered ω rocking curves (RCs) obtained after the XRD instrument is aligned to the (1 1 1) plane of NbN. FWHM values of symmetric RCs around NbN 1 1 1 reflection decrease monotonically from 76″ on 0.5° miscut substrate to 20″ on 10° miscut substrate, indicating a reduction in defects such as threading dislocations, mosaicity, and, to a lesser extent, point defects due to microstrain. As shown later using STEM images, it is difficult to identify the type of defects being reduced in our films. NbN films on substrates with same miscut show no such difference in RC FWHM values as shown in the supplementary material, Fig. S5.

Figures 4(a)–4(c) show the STEM images of NbN on sapphire with 0.5° miscut at different magnifications, and Figs. 4(d)–4(f) for sapphire with 10° miscut. NbN was found to have around 10 nm critical thickness on c-sapphire irrespective of the substrate miscut as shown in Figs. 4(a) and 4(d). Above this critical thickness, columnar growth of NbN is observed. The magnified images in Figs. 4(b) and 4(e) prove the epitaxial and single crystal nature of the NbN film close to the NbN/sapphire interface within the critical thickness. Such epitaxial nature is crucial for the Nagai tilt and miscut mechanism. These NbN films on different miscut substrates do not have surface atomic

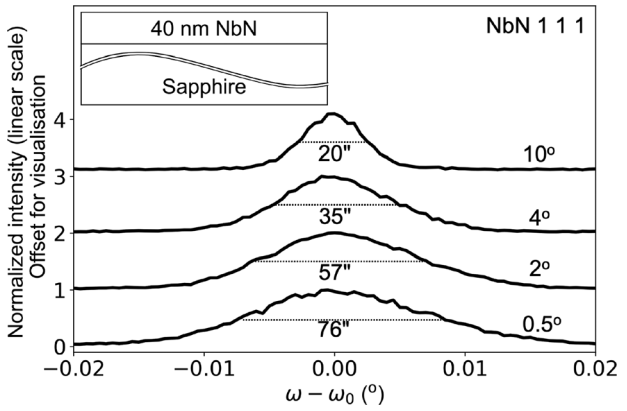

FIG. 3. Normalized ω rocking curves (RCs) around the NbN 1 1 1 reflection show decreasing FWHM with increasing miscut angle of the substrate, the FWHM value of each RC is indicated in arcsecs (″) [3600 arcsecs (″) = 1 degree (°)].

steps as shown in the supplementary material, Fig. S6(a). We attribute this to the three-dimensional growth mode of NbN at the growth temperature of 600 °C.[4] The monotonic trend of increasing surface roughness of NbN with increasing substrate miscut shown in the supplementary material, Fig. S6(b), is still consistent with the miscut mechanism proposed by Nagai.

The angular shift in the NbN (1 1 1) planes with respect to the NbN/sapphire interface in Figs. 4(b) and 4(e) has two components—the substrate miscut μ and the Nagai tilt α as shown in Fig. 1. C-plane sapphire has an inter-planar spacing $d_s = 0.216$ nm and the NbN (1 1 1) planes have an inter-planar spacing $d_f \simeq 0.254$ nm. Therefore, according to the Nagai tilt model, for $\mu = 0.5°$, $\alpha = 0.09°$, and for $\mu = 10°$, $\alpha = 1.78°$. The values obtained from the STEM images, for $\mu = 0.5°$, $\alpha \simeq 0.1°$, and for $\mu = 10°$, $\alpha \simeq 2°$, match closely with the Nagai tilt model.

The columnar grains in the NbN films make it difficult to quantify, using STEM images, the reduction in defects as interpreted from the reduction in RC FWHM with increasing substrate miscut. The STEM images in Figs. 4(a) and 4(d) of NbN on 0.5°, 10° miscut substrate, respectively, show similarities in terms of column grain sizes and lack of mosaicity. Additionally, decreasing the FMHM of RCs due to reduction in point defects such as N-vacancies is consistent with the $2\theta - \omega$ XRD results.

Misfit dislocations of density $\sim 1.6 \times 10^{12}/\text{cm}^2$ (assuming a 50 nm projection thickness) are observed to form at the sapphire/NbN interface. This is consistent with the fact that the thickness of coherently strained NbN is $h_c \simeq 0.1$ nm as estimated from the simplified Matthews–Blakeslee (MB) equation, $h_c = \frac{b}{4\pi f(1+\nu)}\left[\ln\left(\frac{h_c}{b}\right) + 1\right]$.[27] This simplified MB equation is valid only for the edge-type misfit dislocations in the plane of NbN/sapphire interface that belong to the $[1\,\bar{1}\,0](1\,1\,1)$ slip system, which is the most common slip system in the rock salt structure.[21] The Burgers vector magnitude, $b = 0.311$ nm for NbN, $f = 11.7\%$ is the lattice mismatch between NbN and sapphire when $[1\,1\,\bar{2}]$ of NbN is parallel to [1 0 0] of sapphire as in our films, and ν is the Poisson ratio of NbN, taken to be 0.33. The density and periodicity of these misfit dislocations are independent of the substrate miscut as denoted by the yellow dislocation symbols in Figs. 4(c) and 4(f).

The experimental verification of the actual mechanism leading to improved XRD metrics of NbN on large miscut sapphire requires further work. We hypothesize that the reduction in N-vacancies is the predominant cause. This may be due to Nagai tilt in the epitaxial films. Due to this tilt, the NbN growth front is tilted away from the (1 1 1) planes. Incidentally, (1 1 1) planes of rock salt structures are the most densely packed. The diffusion coefficient of N into the film may be expected to increase due to this tilt. The effect of structural improvement on the transport properties is also investigated in this study. Figure 5(a) is a plot of room temperature resistivity of the NbN films on miscut sapphire substrates measured in a Van der Pauw configuration. Despite the evidence of structural improvement with higher miscut substrates, all the films showed very similar room temperature resistivity with no apparent trend probably due to electron–phonon scattering limited transport at 300 K.

The temperature-dependent resistivity shown in Fig. 5(b) was normalized to the room temperature resistivity for each miscut. The inset in Fig. 5(b) shows the superconducting transition temperature. T_c increases marginally by 0.4 K with increasing miscut. The

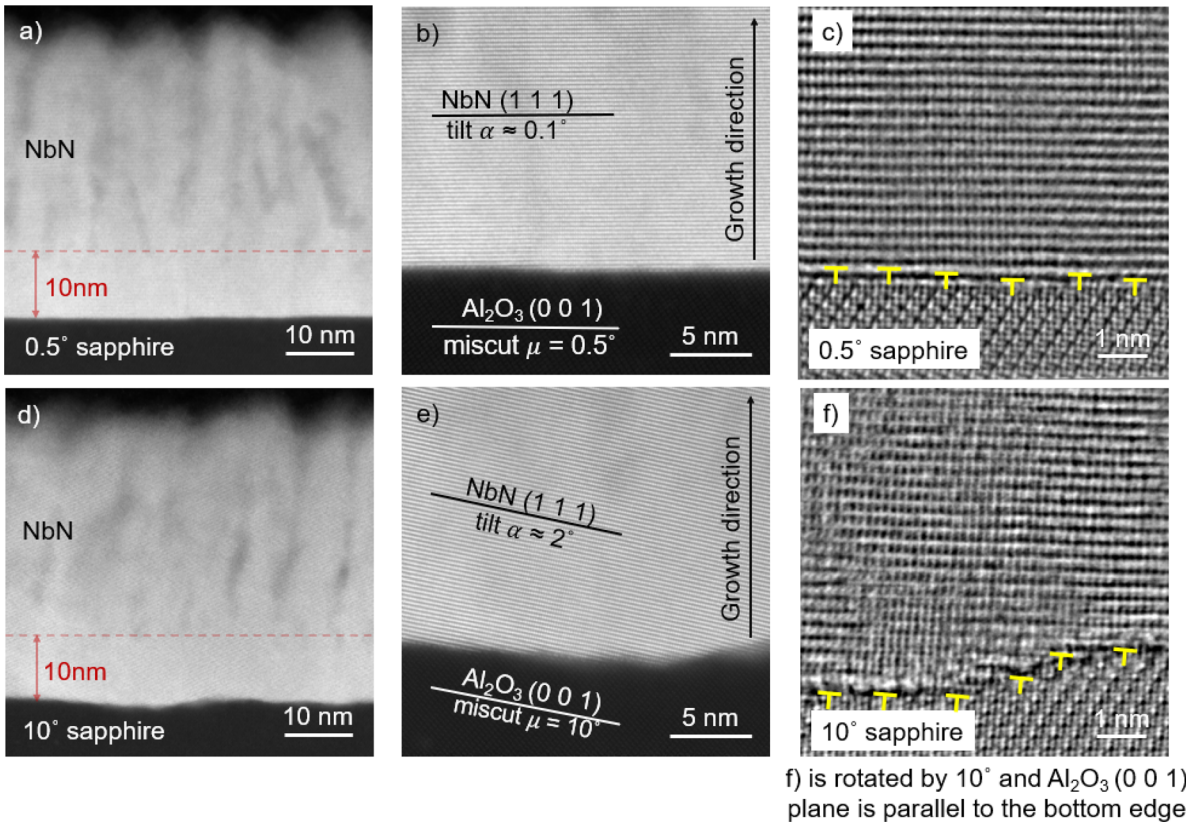

FIG. 4. (a) and (d) Wide field-of-view ADF-STEM images of NbN on 0.5° and 10° miscut sapphire, respectively. Both samples show a clean epitaxial NbN film in the initial 10 nm followed by columnar growth. (b) and (e) Atomic resolution ADF-STEM images of the NbN to 0.5° and 10° miscut sapphire interface, respectively. The sapphire interface is aligned normal to the growth direction, and the NbN (1 1 1) planes prefer to be parallel to the sapphire (0 0 1) planes. (c) and (f) Atomic resolution iDPC image of the NbN to 0.5° and 10° miscut sapphire interface aligning the sapphire (0 0 1) plane. The iDPC captures the tilts and disorder within the NbN that leads to blur in the image. The misfit dislocation between NbN and sapphire is noted in yellow across the interface. Both samples show a similar dislocation density ~1.6×10^{12}/cm^2 (assuming a 50 nm projection thickness). The high dislocation density reflects the large difference and lattice constant between the sapphire and relaxed NbN.

temperature-dependent resistivity curves of the control set shown in the supplementary material, Fig. S7, have less than 0.2 K variance in T_c. This suggests that the T_c increase with increasing substrate miscut is not an artifact. It must be noted that these measurements were done fresh after the growth and may not be reproducible after exposure to atmosphere over extended periods of time due to the possibility of impurity diffusion along column boundaries.[28] The marginal increase in T_c can also be explained with our hypothesis of increasing N:Nb

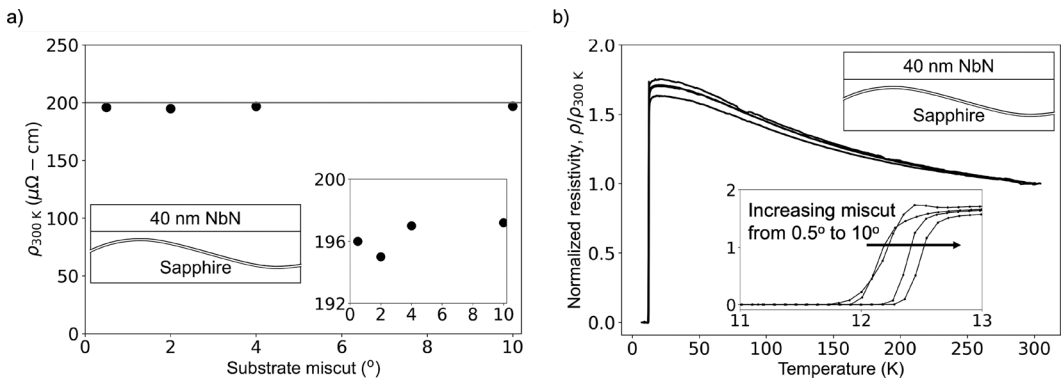

FIG. 5. (a) Room temperature resistivity of NbN films vs substrate miscut angle showing no impact of the substrate miscut. (b) Marginal increment in NbN film's superconducting critical temperature, T_c, with increasing miscut angle of the sapphire substrate is seen from the normalized resistance vs temperature curve.

ratio with increasing substrate miscut. There is extensive literature on the positive correlation between T_c and N:Nb ratio in NbN_x for $0.5 \leq x \leq 1$.[5–7] Other effects on T_c such as thickness[11,29] and phase-purity[4,9] are not applicable to our films as they are grown together in an ultra-high vacuum chamber and are phase-pure.

From the inset of Fig. 5(b), the residual resistivity ratio (RRR), $\rho_{300\,K}/\rho_{13\,K}$, increases marginally from 0.59 for NbN on 0.5° and 4° miscut to 0.62 for NbN on 10° miscut. An increase in RRR is a typical signature of reduced defects. An exception in the RRR trend is that of 2° miscut, with an RRR of 0.57, which cannot be explained based on the structural results presented in this study and may be due to competing scattering mechanisms.

In conclusion, we employed large miscut (up to 10°) sapphire substrates and observed an improvement in structural quality of NbN films as assessed by XRD. We have also observed that irrespective of the substrate miscut, around 10 nm of highly crystalline NbN grows on c-plane sapphire. Beyond this thickness, the NbN films relax into columns. These columns have boundaries which can potentially allow impurities like O and C atoms to diffuse in from the surface. The cause for the structural improvement with the miscut angle is not fully understood and requires further work. Reduction in N-vacancies with increasing substrate miscut is proposed to be the leading candidate. Growth of transition metal nitrides which do not have columnar structure on c-plane sapphire can help understand which defects are reduced by employing large miscuts.

This study points to a number of avenues to pursue. The first is to compare the thick (>10 nm) and thin (<10 nm) NbN films epitaxially grown on c-sapphire in terms of transport and structural properties. The choice of miscut direction in this study was m-axis of sapphire. A different choice, say, a-axis, of miscut direction might be worth studying to verify the universality of this study. Also, a 32.4° miscut toward m-axis would correspond to the r-plane. The results from this study also indicate that r-plane sapphire should be explored for epitaxial NbN growth.

See the supplementary material for data supporting the phase purity of the NbN films presented in the main text and for data collected from the control set of samples.

This work is supported by the AFOSR/LPS program Materials for Quantum Computation (MQC) as part of the EpiQ team under Award No. FA9550-23-1-0688 monitored by Dr. Ali Sayir of AFOSR and Dr. Erin Cleveland of LPS, and partially by an ONR grant (No. N00014-22-1-2633) monitored by Dr. Paul Maki. The authors acknowledge the use of facilities and instrumentation supported by NSF through the Cornell University Materials Research Science and Engineering Center (DMR-1719875).

AUTHOR DECLARATIONS

Conflict of Interest

The authors have no conflicts to disclose.

Author Contributions

Anand Ithepalli: Conceptualization (equal); Data curation (lead); Formal analysis (lead); Methodology (equal); Project administration (equal); Visualization (equal); Writing – original draft (lead); Writing – review & editing (equal). **Saumya Vashishtha:** Data curation (supporting); Formal analysis (supporting); Validation (supporting); Visualization (supporting). **Naomi Pieczulewski:** Data curation (supporting); Formal analysis (supporting); Validation (supporting); Visualization (supporting); Writing – review & editing (supporting). **Qiao Liu:** Formal analysis (supporting); Methodology (supporting). **Amit Rohan Rajapurohita:** Formal analysis (supporting). **Matthew Barone:** Methodology (supporting). **Darrell Schlom:** Funding acquisition (supporting); Methodology (supporting); Resources (equal); Supervision (supporting). **David A. Muller:** Funding acquisition (supporting); Investigation (supporting); Methodology (supporting); Supervision (supporting). **Huili Grace Xing:** Funding acquisition (supporting); Resources (equal); Supervision (supporting); Writing – review & editing (supporting). **Debdeep Jena:** Conceptualization (equal); Formal analysis (equal); Funding acquisition (lead); Project administration (equal); Resources (equal); Supervision (lead); Validation (equal); Writing – review & editing (equal).

DATA AVAILABILITY

The data that support the findings of this study are available from the corresponding author upon reasonable request.

REFERENCES

[1]F. Aschermann and J. Kramer, Physica Z **42**, 349 (1941).
[2]G. Brauer, "Nitrides, carbonitrides and oxynitrides of niobium," J. Less Common Met. **2**, 131 (1960).
[3]B. W. Roberts, "Survey of superconductive materials and critical evaluation of selected properties," J. Phys. Chem. Ref. Data **5**, 581 (1976).
[4]J. G. Wright, H. G. Xing, and D. Jena, "Growth windows of epitaxial NbN_x films on c-plane sapphire and their structural and superconducting properties," Phys. Rev. Mater. **7**, 074803 (2023).
[5]A. Linde, R.-M. Marin-Ayral, F. Bosc-Rouessac, and V. Grachev, "Effect of nitrogen to niobium atomic ratio on superconducting transition temperature of δ-NbN x powders," Int. J. Self. Propag. High. Temp. Synth. **19**, 9 (2010).
[6]S. Kalal, M. Gupta, and R. Rawat, "N concentration effects on structure and superconductivity of NbN thin films," J. Alloys Compd. **851**, 155925 (2021).
[7]V. Buscaglia, F. Caracciolo, M. Ferretti, M. Minguzzi, and R. Musenich, "Effect of pressure on the composition and superconducting Tc value of NbN prepared by combustion synthesis," J. Alloys Compd. **266**, 201 (1998).
[8]T. Yamashita, K. Hamasaki, and T. Komata, "Epitaxial growth of NbN on MgO film," in *Advances in Cryogenic Engineering Materials* (Springer, 1986) pp. 617–626.
[9]D. S. Katzer, N. Nepal, M. T. Hardy, B. P. Downey, D. F. Storm, E. N. Jin, R. Yan, G. Khalsa, J. Wright, A. C. Lang *et al.*, "Molecular beam epitaxy of transition metal nitrides for superconducting device applications," Phys. Status Solidi A **217**, 1900675 (2020).
[10]A. Kobayashi, S. Kihira, T. Takeda, M. Kobayashi, T. Harada, K. Ueno, and H. Fujioka, "Crystal-Phase Controlled Epitaxial Growth of NbNx Superconductors on Wide-Bandgap AlN Semiconductors," Adv. Mater. Interfaces **9**, 2201244 (2022).
[11]J. G. Wright, C. S. Chang, D. A. Muller, H. G. Xing, and D. Jena, "Structural and electronic properties of nbn/gan junctions grown by molecular beam epitaxy," APL Mater. **10**, 051103 (2022).
[12]J. Wright, C. Chang, D. Waters, F. Lüpke, R. Feenstra, L. Raymond, R. Koscica, G. Khalsa, D. Muller, H. G. Xing *et al.*, "Unexplored MBE growth mode reveals new properties of superconducting NbN," Phys. Rev. Mater. **5**, 024802 (2021).
[13]T. Roch, M. Gregor, S. Volkov, M. Čaplovičová, L. Satrapinskyy, and A. Plecenik, "Substrate dependent epitaxy of superconducting niobium nitride thin films grown by pulsed laser deposition," Appl. Surf. Sci. **551**, 149333 (2021).
[14]M. J. Sowa, Y. Yemane, J. Zhang, J. C. Palmstrom, L. Ju, N. C. Strandwitz, F. B. Prinz, and J. Provine, "Plasma-enhanced atomic layer deposition of superconducting niobium nitride," J. Vac. Sci. Technol. A **35**, 01B143 (2016).

[15]D. Wang, Y. Wu, N. Pieczulewski, P. Garg, M. C. Pace, C. Bøttcher, B. Mazumder, D. A. Muller, and H. X. Tang, "All-nitride superconducting qubits based on atomic layer deposition," arXiv:2511.08931 (2025).
[16]C. R. H. McRae, H. Wang, J. Gao, M. R. Vissers, T. Brecht, A. Dunsworth, D. P. Pappas, and J. Mutus, "Materials loss measurements using superconducting microwave resonators," Rev. Sci. Instrum. **91**, 091101 (2020).
[17]H. Nagai, "Structure of vapor-deposited $Ga_xIn_{1-x}As$ crystals," J. Appl. Phys. **45**, 3789 (1974).
[18]S. Rathkanthiwar, M. B. Graziano, J. Tweedie, S. Mita, R. Kirste, R. Collazo, and Z. Sitar, "Crystallographic tilt in aluminum gallium nitride epilayers grown on miscut aluminum nitride substrates," Phys. Rapid Res. Lett. **17**, 2200323 (2023).
[19]M. Pristovsek, I. Furuhashi, and P. Pampili, "Growth of N-Polar (000-1) GaN in metal–organic vapour phase epitaxy on sapphire," Crystals **13**, 1072 (2023).
[20]A. Zauner, J. Weyher, M. Plomp, V. Kirilyuk, I. Grzegory, W. van Enckevort, J. Schermer, P. Hageman, and P. Larsen, "Homo-epitaxial gan growth on exact and misoriented single crystals: Suppression of hillock formation," J. Cryst. Growth **210**, 435 (2000).
[21]A. Farhadizadeh, J. Salamania, M. Sortica, D. Primetzhofer, and M. Odén, "Structure evolution during growth of epitaxial NbN films on Al2O3 (0006) deposited by magnetron sputtering and its impact on electrical properties," J. Cryst. Growth **656**, 128094 (2025).
[22]S. A.-A. Jabir and K. H. Harbbi, "A comparative study of Williamson-Hall method and size-strain method through X-ray diffraction pattern of cadmium oxide nanoparticle," AIP Conf. Proc. **2307**, 020015 (2020).
[23]P. Tatarczak, H. Turski, K. P. Korona, E. Grzanka, C. Skierbiszewski, and A. Wysmołek, "Optical properties of N-polar GaN: The possible role of nitrogen vacancy-related defects," Appl. Surf. Sci. **566**, 150734 (2021).
[24]N. Terao, "New phases of niobium nitride," J. Less Common Met. **23**, 159 (1971).
[25]R. Berger, W. Lengauer, and P. Ettmayer, "The γ-$Nb_4N_{3\pm x}$→δ-NbN_{1-x} phase transition," J. Alloys Compd. **259**, L9 (1997).
[26]V. I. Ivashchenko, P. E. A. Turchi, and E. I. Olifan, "Phase stability and mechanical properties of niobium nitrides," Phys. Rev. B **82**, 054109 (2010).
[27]J. Matthews and A. Blakeslee, "Defects in epitaxial multilayers: I. Misfit dislocations," J. Cryst. Growth **27**, 118 (1974).
[28]A. M. Chornous, L. Dekhtyaruk, T. Govorun, and A. O. Stepanenko, "Influence of diffusing impurities on the electrical conductivity of single-crystal and polycrystalline metal films," Metallofiz. Noveishie Tekhnol. **29**, 249 (2007).
[29]N. Cucciniello, D. Lee, H. Y. Feng, Z. Yang, H. Zeng, N. Patibandla, M. Zhu, and Q. Jia, "Superconducting niobium nitride: A perspective from processing, microstructure, and superconducting property for single photon detectors," J. Phys. Condens. Matter **34**, 374003 (2022).